

A Semi-Automated Method for Epileptiform Transient Detection in the EEG of the Fetal Sheep Using Time-Frequency Analysis

Anita C. Walbran, *Student Member, IEEE*, Charles P. Unsworth, *Member, IET*, Alistair J. Gunn, and Laura Bennet

Abstract—Perinatal hypoxia remains a significant cause of brain damage. Currently there are no biomarkers to detect the at risk brain. Recent research, however, suggests that the appearance of epileptiform transients in the first 6-8 hours after hypoxia (the latent phase of injury) are predictive of neural outcome. To quantify this further a key need is to automate EEG signal analysis to aid clinical staff with the vast amounts of complex data to review. In this study, we present a semi-automated method for spike detection in the fetal sheep EEG. The method utilizes the short time Fourier transform and peak separation to extract spikes. The performance of the method was found to be high in sensitivity and selectivity over 3 distinct time points.

I. INTRODUCTION

HYPOXIA before or during birth is a significant cause of brain damage [1]. Brain damage is an evolutionary process, allowing windows of opportunity for treatment. Neuroprotective treatments appear to be most effective if started in the latent phase of recovery: the first 6 to 8 hours after the end of the insult, with efficacy lost if started after this time [2], [3]. Birth itself cannot be taken as time zero, since the insult may have occurred well before birth. Thus, for treatments to be effective, it is critical to determine which phase of injury the brain is in. However, there are no specific biomarkers for evolving brain injury in the latent phase [4].

Measurement of the electroencephalogram (EEG) has the potential to allow rapid bedside assessment of the brain, and features of the EEG such as amplitude suppression and high amplitude seizures can predict long-term injury [3]. However, these features are not predictive in the latent phase. Recent studies suggest that there are more subtle features of the EEG that may be pathological and potentially

predictive of outcome [5]–[8]. These features are defined as epileptiform transients. They are typically low amplitude, high frequency, <400 ms events defined as spikes, sharps and slow waves occurring singly or as complexes [9], [10].

Increasingly, neonatal monitoring utilizes a reduced 2-4 lead EEG configuration at 512 Hz [11]. However, such data collection leaves clinical staff vast amounts of complex data to review and quantify. The key need is to automate signal analysis to enable real-time use.

The aim of this study was to develop a simple yet robust semi-automated spike detection algorithm which requires minimal assistance from a user, to accurately assess 3 specific time points during the latent phase in a preterm fetal sheep model after asphyxia *in utero*. We report our preliminary findings in one sheep fetus.

II. METHODS

A. Data Acquisition

All procedures were approved by the Animal Ethics Committee of the University of Auckland, New Zealand. A singleton Romney/Suffolk sheep fetus was instrumented under general anesthesia, using sterile techniques at 97-98 days of gestation (term = 147 days [7]). A catheter was placed in the fetal brachial artery for blood sampling. Two pairs of electroencephalogram (EEG) electrodes (AS633-7SSF, Cooner Wire Co., US) were placed on the dura over the parasagittal parietal cortex (5 mm and 10 mm anterior to bregma and 5 mm lateral) and secured with cyanoacrylate glue. A reference electrode was sewn over the occiput. An inflatable silicone occluder was also placed around the umbilical cord of the fetus (In Vivo Metric, US). The fetus was returned to the uterus and the ewe and fetus allowed to recover for 5 days. During recovery, the sheep was housed with companion sheep in separate metabolic cages and given free access to water and food. Antibiotics were administered daily intravenously to the ewe (600 mg Benzylpenicillin Sodium; 80 mg Gentamicin). Fetal arterial blood was taken daily from the brachial artery for blood gas analysis for the assessment of fetal health.

The experiment was conducted at 103 days of gestation (term is 147 days, ~ 27-30 weeks human brain maturation) [12]. Fetal asphyxia was induced by rapid inflation of the umbilical cord occluder for 25 min with isotonic saline of a defined volume known to completely inflate the occluder [7]. Successful occlusion was confirmed by fetal blood samples taken for pH and blood gases (Ciba-Corning

Manuscript received April 23, 2009. This work was supported by a Top Achiever Doctoral Scholarship from the Tertiary Education Commission, New Zealand and the Health Research Council, New Zealand.

A. C. Walbran is with the Department of Engineering Science, The University of Auckland, Auckland 1010, New Zealand. (phone: +64-9-373-7599 ext 87056; fax: +69-9-373-7468; e-mail: a.walbran@auckland.ac.nz).

C. P. Unsworth is a Senior Lecturer at the Department of Engineering Science, The University of Auckland, Auckland 1010, New Zealand. (e-mail: c.unsworth@auckland.ac.nz).

L. Bennet is an Associate Professor in the Department of Physiology, Faculty of Medical and Health Sciences, The University of Auckland, Private Bag 92019, Auckland, New Zealand (email: l.bennet@auckland.ac.nz).

A. J. Gunn is a Professor in the Department of Physiology, Faculty of Medical and Health Sciences, The University of Auckland, Private Bag 92019, Auckland, New Zealand (email: aj.gunn@auckland.ac.nz).

Diagnostics 845 Blood Gas Analyzer/Co-oximeter, US), and observation of a rapid flattening of the EEG.

The signals from EEG electrodes were channeled via leads through individual unity-gain head-stages for reduction of noise by selective signal amplification ($\times 10,000$) and low-pass filtered with a sixth order low-pass Butterworth anti-aliasing filter, with the -3 decibel (dB) point set to a cut-off frequency of 50 Hz. The signals were then digitized by computer at a sampling rate of 512 Hz. Fetal EEG was then monitored for 8 hours after asphyxia.

B. Epoch analysis

For this analysis 3 specific time points during the latent phase were chosen to analyze spike activity: 0.5 hour (h), 3.0 h, and 6.2 h after asphyxia. These time points were chosen to determine spike activity during 1) the early-latent recovery phase, during which time there is partial recovery of cerebral oxidative metabolism [4], 2) the mid-latent recovery phase, at which time we have previously seen maximal transient activity and the beginning of progressive metabolic deterioration [4]-[6], [13], and 3) the late-latent recovery phase, when transient activity decreases just prior to the onset of stereotypic evolving seizures and the transition of brain cells from being reversibly to irreversibly injured occurs [4].

C. Waveform analysis

We identified all spikes in a 10 minute segment of the left EEG at the 3 specific time points during the latent phase. A spike was defined as having a sharp outline and duration of less than 70 ms with an amplitude greater than 20 μV , typically superimposed on a suppressed EEG background [10].

D. Time-Frequency Analysis

Time-frequency analysis [14] consists of a series of signal processing techniques that allow one to process non-stationary signals whose constituent frequencies vary with time. Such techniques are an extension of Fourier analysis [14] where the signals are stationary and frequencies are assumed to be constant with time. Hence, time-frequency analysis lends itself naturally to real world signals such as biomedical signals like the EEG and ECG which are both time dependent and highly non-stationary. Several time domain [15]-[19] and frequency domain [20]-[22] spike detection methods have been presented in the literature for human EEG. In this paper, we perform semi-automated spike detection in the EEG of preterm fetal sheep.

To perform the initial mass spike detection, we employ a time-frequency based method, by way of the discrete short-time Fourier transform (STFT),

$$X(m, k) = \sum_{n=1}^N x[n](W[n-k]e^{-jnm/N}) \quad (1)$$

where $X(m, k)$ is the observed spectral content for a discrete EEG signal $x[n]$ at data index n , N is the data length, $W[n-k]$

is the window function at position k and $e^{-jnm/N}$ is a family of sinusoidal basis functions with m specifying the frequency of an individual sinusoid in the family. Once the times of the spikes have been located they are then further classified into single spikes, multiple-spikes and non-resolvable spikes by a series of simple time based measurements. Fig. 1, shows schematically the process of spike detection.

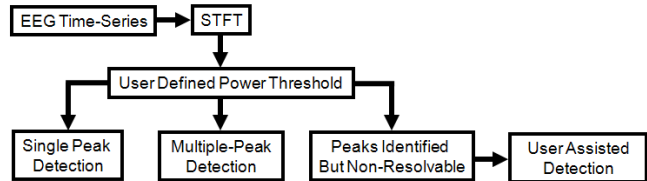


Fig. 1. Process of spike detection.

Firstly, the STFT of the raw EEG data was produced. This employed a hamming window of length 18 and window overlap of 16 data points. The window was zero-padded to the next power of two then zero-padded to twice its resulting length, giving a frequency resolution of 0.67Hz. This was performed for 10 minute data segments at each of the 3 specific time points during the latent recovery phase.

For each time step in the STFT, the average power for frequencies greater than the minimum frequency of a spike wave was calculated and stored in an array. By way of the STFT, the user then defined a power threshold necessary to extract the high frequency peaks corresponding to spikes in the time domain, from the average power array. In order to extract the high power peaks, a window with length equivalent to that of a 70 ms spike was slid across the average power array. If the maximum of all data points within this window was greater than the power threshold, then the power value of the point in the middle of the sliding window was retained, otherwise it was set to zero. This method was used instead of a straight thresholding approach to ensure that the start and end of each peak was captured and not just the middle portion of the peak.

On examination some multiple peaks were found that corresponded to two or more spikes that occur very closely in time. To separate these multiple peaks, the algorithm examined the gradients of the peaks. A window consisting of 3 points was slid over the peaks detected after power thresholding. The minimum of the points in the window was examined. By tracing the minimum, an indication of whether the peak was increasing or decreasing in gradient was obtained. If the gradient decreased then increased before the end of the peak was reached, then that peak was termed a multiple peak. In order to separate the multiple peaks the minimum point indicating the overlap of the multiple peaks was set to zero (Fig. 2A and 2B).

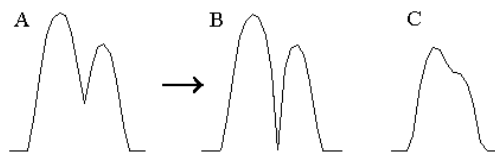


Fig. 2. A: double peak; B: separated peaks; C: non-resolvable peak.

This method of peak separation worked well for multiple peaks where there were distinct peaks (Fig. 2A). However, in some cases, multiple spikes were so close in time that they could not be resolved. The only clue was that the signal had one main peak and one or more small auxiliary peak on the side, suggesting the signal contained multiple non-resolvable spikes (Fig. 2C).

In addition, such non-resolvable peaks had a slightly longer duration than the peaks containing a single spike. To deal with this special case, the start and end times of the peaks identified were recorded and used to calculate the average duration of the peaks. If the duration of a peak was greater than one and a half times the average duration, then it was plotted alongside its corresponding section of EEG in the time domain. The user was then asked to confirm how many spikes were contained within the peak.

The peaks detected from the analysis were then compared with the peaks identified by the authors. As the peaks detected in the frequency domain were a lot wider than the corresponding spikes in the time domain, the end point of the peak detected in the frequency domain was compared with the start point of the spike in the time domain as they lined up most accurately.

E. Performance Evaluation

The performance of this algorithm was evaluated by quantifying the following parameters [23]:

- 1) *True positive (TP)*: the algorithm identifies a spike that has also been identified by the expert.
- 2) *False positive (FP)*: The algorithm identifies a spike that has not been identified by the expert.
- 3) *False negative (FN)*: The algorithm fails to detect a spike identified by the expert.

Using the above parameters, the following performance measures of sensitivity (SEN), the ability of the algorithm to detect spikes (2), and selectivity (SEL), the ability of the algorithm to reject false detections of spikes (3) were calculated [23].

$$SEN = TP / (TP + FN) \times 100 \quad (2)$$

$$SEL = TP / (FP + FN) \times 100 \quad (3)$$

III. ALGORITHM PERFORMANCE

A typical section of EEG in the early-latent recovery phase is shown in Fig. 3A with spikes identified by the authors marked with an arrow. The STFT of this section of data is shown in Fig. 3B. As expected, the high frequency bands of high power in the STFT align with the high frequency spikes in the time domain. The peaks, as detected by the algorithm in the frequency domain, are shown Fig. 3C. Fig. 3D shows the peaks after the double peak has been separated automatically by the algorithm. Vertical lines correspond to the location of the spikes identified by the authors in the time domain.

We identified 212, 88 and 74 spikes for the early-latent,

mid-latent and late-latent recovery phases respectively. Table I shows the performance of the algorithm in terms of sensitivity and selectivity for increasing power thresholds. User assistance for detecting non-resolvable peaks was required for ~10% of peaks detected and increased sensitivity and selectivity on average by 6% and 1% respectively compared to the method without user assistance.

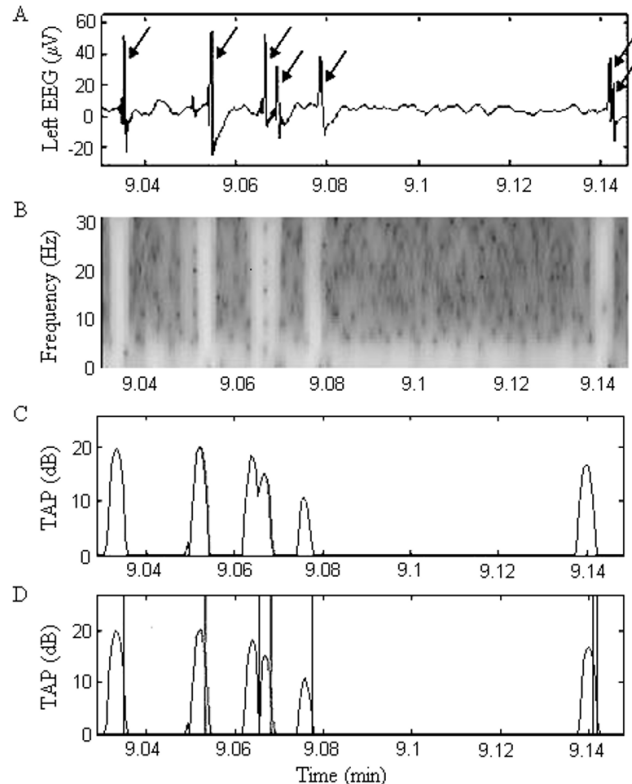


Fig. 3. A: Typical EEG segment with spikes identified by the authors marked with an arrow. B: STFT of the corresponding segment. Light bands represent high power. C: Peaks detected by the algorithm prior to separation of multiple peaks. D: Peaks after separation. Vertical lines correspond to the spikes identified by the authors. TAP=Thresholded average power.

TABLE I
PERFORMANCE RESULTS

	Early-latent		Mid-latent		Late-Latent	
Power threshold	SEN	SEL	SEN	SEL	SEN	SEL
5	85.4	73.6	94.3	81.3	81	58.3
6	84.9	76.3	93.2	85.4	79.7	61.5
7	82.1	78.4	89.8	88.8	78.4	71.6
8	77.4	82.8	83	92.4	73	76.1

Results show the sensitivity (SEN) and selectivity (SEL) of the method for increasing power thresholds.

The results show that for an increase in power threshold the sensitivity of the algorithm decreased and the selectivity increased. This is due to lower thresholds allowing more peaks to be detected, therefore increasing the sensitivity but also increasing the number of false positives. Therefore, a balance between sensitivity and selectivity must be

achieved. We believe that the algorithm resulted in the best overall performance at a power threshold of 7. This gives a sensitivity and selectivity of 82.1% and 78.4% respectively for the early-latent recovery phase, 89.8% and 88.8% respectively for the mid-latent recovery phase and 78.4% and 71.6% respectively for the late-latent recovery phase.

IV. DISCUSSION

A method for semi-automated detection of spikes in a fetal sheep EEG has been presented and its sensitivity and selectivity compared at 3 specific time points during the latent phase of recovery (the period during which current neuroprotective treatments must be started for efficacy). The sensitivity and selectivity for this particular data set was highest during the mid-latent phase, and lowest during the late-latent phase. Lower performance results in the late-latent phase are due to high frequency, low amplitude bursts occurring as the background EEG becomes less suppressed and increasingly unstable prior to the onset of high amplitude stereotypic evolving seizures [4]. The high frequency bursts appear as areas of high power in the STFT so increase the number of false positives.

The method has proved to be simple and robust and requires ~10% intervention by a user to identify non-resolvable multiple-spikes. It was noted that this method detects some spikes that have an amplitude less than the 20 μ V threshold. This is due to the spikes still being high frequency so they appear as high power in the STFT.

The method distinguishes between spike waves and sharp waves where the sharp wave is towards the longer end of its 70-200 ms duration by definition. Our intentions are to extend the method to distinguish between spikes and sharp waves with durations towards the faster end of the 70-200 ms duration, thus enhancing the utility of transient assessment in determining the phase of injury that the brain is in. Future work will also be focused on utilizing methods that allow flexibility in the time-frequency resolution. The algorithm will be tested and further refined in a large cohort of animals in the paradigm. Ultimately, it is our goal to develop a fully automated spike and sharp wave detection method and apply it to the human infant.

ACKNOWLEDGMENT

We are grateful for the help of EEG technician Mark Gunning from the Department of Physiology, The University of Auckland.

REFERENCES

- [1] J. E. Lawn, S. Cousins and J. Zupan. 4 million neonatal deaths: when? Where? Why? *Lancet* 365(9462). pp. 891-900, 2005.
- [2] P. D. Gluckman, A. J. Gunn and J. S. Wyatt. Hypothermia for neonates with hypoxic-ischemic encephalopathy. *New England Journal of Medicine* 354(15.) pp. 1643-5, 2006.
- [3] A. J. Gunn, J. S. Wyatt, A. Whitelaw, D. Azzopardi, J. Barks, R. Ballard, A. D. Edwards, D. M. Ferriero, P. D. Gluckman, R. A. Polin, D. M. Robertson and M. Thoresen, on behalf of the CoolCap Study Group. Therapeutic hypothermia changes the prognostic value of clinical evaluation of neonatal encephalopathy. *Journal of Pediatrics* 152(1). pp. 55-58, 2008.
- [4] A. J. Gunn, and L. Bennet. Timing of injury in the fetus and neonate. *Current Opinion in Obstetrics and Gynecology* 20(2). pp. 175-181, 2008.
- [5] S. George, A. J. Gunn, J. A. Westgate, C. Brabyn, J. Guan, and L. Fetal heart rate variability and brainstem injury after asphyxia in preterm fetal sheep. *American Journal of Physiology. Regulatory Integrative and Comparative Physiology* 287(4). R925-R933, 2004.
- [6] L. Bennet, J. M. Dean, G. Wassink, and A. J. Gunn. Differential effects of hypothermia on early and late epileptiform events after severe hypoxia in preterm fetal sheep. *Journal of Neurophysiology* 97(1). pp. 572-8, 2007.
- [7] J. M. Dean, S. A. George, G. Wassink, A. J. Gunn, and L. Bennet. Suppression of post hypoxic-ischemic EEG transients with dizocilpine is associated with partial striatal protection in the preterm fetal sheep. *Neuropharmacology* 50(4). pp. 491-503, 2006.
- [8] A. Sofue, A. Okumura, F. Hayakawa, and K. Watanabe. Sharp waves in preterm infants with periventricular leukomalacia. *Pediatric Neurology* 29(3). pp. 214-7, 2003.
- [9] C. D. Binnie. General characteristics of the EEG. In: Neonatal and paediatric clinical neurophysiology, Pressler RM, ed, Ed, Ch, pp. 7-109. Edinburgh: Churchill Livingstone/Elsevier, 2007.
- [10] M. Scher. Neonatal seizures: an expression of fetal or neonatal brain disorders. In: Fetal and Neonatal Brain Injury. Mechanisms, management and the risks of practice (Stevenson DK, Benitz WE, Sunshine P, eds), 2nd ed., Ch, pp. 735-784. Cambridge: Cambridge University Press, 2003.
- [11] G. Macdonald. Long-term EEG monitoring in the Neonatal Intensive Care Unit. *Conf Proc IEEE Eng Med Biol Soc* 3. pp. 2483-5, 2005.
- [12] G. H. McIntosh, K. I. Baghurst, B. J. Potter, and B. S. Hetzel. Foetal brain development in the sheep. *Neuropathol Appl Neurobiol* 5. pp. 103-114, 1979.
- [13] S. C. Roth, A. D. Edwards, E. B. Cady, D. T. Delpy, J. S. Wyatt, D. Azzopardi *et al.* Relation between cerebral oxidative metabolism following birth asphyxia, and neurodevelopmental outcome and brain growth at one year. *Dev Med Child Neurol* 34. pp. 285-295, 1992.
- [14] S. M. Kay, and S. T. L. Marple Jr. Spectrum analysis – A modern perspective.
- [15] J. Gotman, and P. Gloor. Automatic recognition and quantification of interictal epileptic activity in the human scalp EEG. *Electroenceph clin Neurophysiol* 41. pp. 513-529, 1976.
- [16] H. S. Liu, T. Zhang, and F.S. Yang. A multistage, multimethod approach for automatic detection and classification of epileptiform EEG. *IEEE Transactions on Biomedical Engineering*, 49(12). pp. 1557 – 1566, 2002.
- [17] M. B. Malarvili, H. Hassanpour, M. Mesbah, and B. Boualem. A histogram-based electroencephalogram spike detection. In: Signal processing and its applications 2005. Proceedings of the Eight International Symposium on. I. pp. 207-210, August, 2005.
- [18] A. T. Tzallas, V. P. Oikonomou, and D. I. Fotiadis. Epileptic spike detection using a kalman filter based approach. In: Engineering in Medicine and Biology Society, 2006. EBMS '06. 28th Annual International Conference of the IEEE, 2006.
- [19] N. Acir, İ. Öztura, M. Kuntalp, B. Baklan, and C. Guzelış. Automatic detection of epileptiform events in EEG by a three-stage procedure based on artificial neural networks. *IEEE Transaction son Biomedical Engineering*, 52(1). pp. 30-40, 2005.
- [20] H. Hassanpour, M. Mesbah, and B. Boashash. EEG spike detection using time-frequency signal analysis. In Acoustics, Speech, and Signal Processing, 2004. Proceedings. (ICASSP '04). IEEE International Conference on. pp. 421-424, 2004.
- [21] T. Kalayci. and O. Ozdamar. Wavelet preprocessing for automated neural network detection of EEG spikes, in IEEE Engineering in Medicine and Biology Magazine. pp. 160-166, 1995.
- [22] S. B. Kim, Y. H. Lee, J.H. Kim and S. I. Kim. Automatic detection of epileptiform activity using wavelet and expert rule base, in Engineering in Medicine and Biology Society, 1998. Proceedings of the 20th Annual International Conference of the IEEE. 1998.
- [23] A. Aarabi, R. Grebe, and F. Wallois. A multistage knowledge-based system for EEG seizure detection in newborn infants. *Clinical Neurophysiology* 118. pp. 2781-2797, 2007.